catalysts

MDPI

Article

In Situ DRIFTS Study of Na-Promoted Pt/ZSM5 Catalysts for H_2-SCR

Stefano Cimino, Elisabetta Maria Cepollaro, Michele Emanuele Fortunato and Luciana Lisi *

Istituto di Scienze e Tecnologie per l'Energia e la Mobilità Sostenibili, CNR, Piazzale Tecchio 80, 80125 Napoli, Italy; stefano.cimino@cnr.it (S.C.); elisabettamaria.cepollaro@stems.cnr.it (E.M.C.); micheleemanuele.fortunato@stems.cnr.it (M.E.F.)
* Correspondence: luciana.lisi@cnr.it

Abstract: Platinum was supported on ZSM5 at loadings from 0.1 to 1 wt% and tested for the Selective Catalytic Reduction of NO with H_2 under excess O_2 in a fixed bed reactor to address the issue of NO_x emission abatement from H_2-fueled internal combustion engines avoiding the additional devices for urea storage and injection. To reduce the undesired NO oxidation to NO_2, which is activated by platinum at T > 200 °C, the 0.1%Pt/ZSM5 catalyst was further promoted with sodium. 5 wt% loading of Na strongly inhibited the NO oxidation while giving only a limited impact on the H_2-SCR activity. Unpromoted and Na-promoted catalysts were characterized by XRD, SEM/EDX, N_2 physisorption, and NH_3-TPD to investigate the morphological, structural, and acid properties; H_2 pulse chemisorption and DRIFTS of CO chemisorption were used to investigate the nature of Pt active species. Steady-state and transient operando DRIFTS experiments under $NO+H_2+O_2$ flow were employed to identify the adsorbed NO_x species interacting with H_2, and reaction intermediates as a function of the reaction conditions. The formation of ammonium intermediates via the reduction of surface nitrate species, playing a key role in H_2-SCR catalyzed by 0.1Pt/ZSM5, was preserved at low Na load whilst NO_2 formation was largely inhibited.

Keywords: H_2-SCR; platinum; zeolite; DRIFT spectroscopy

check for updates

Academic Editor: Anker Degn Jensen

Received: 7 April 2025
Revised: 4 June 2025
Accepted: 13 June 2025
Published: 17 June 2025

Citation: Cimino, S.; Cepollaro, E.M.; Fortunato, M.E.; Lisi, L. In Situ DRIFTS Study of Na-Promoted Pt/ZSM5 Catalysts for H_2-SCR. *Catalysts* **2025**, *15*, 598. https://doi.org/10.3390/catal15060598

Copyright: © 2025 by the authors. Licensee MDPI, Basel, Switzerland. This article is an open access article distributed under the terms and conditions of the Creative Commons Attribution (CC BY) license (https://creativecommons.org/licenses/by/4.0/).

1. Introduction

The transport sector is responsible for a large fraction of CO_2 emissions. To mitigate global warming, in addition to the development of electric vehicles, other solutions, still based on the internal combustion engine (ICE), have been proposed, such as the use of hydrogen as fuel.

Hydrogen is a carbon-free energy carrier and a virtually emission-free fuel, thus representing a good alternative to electric and fuel cell-powered vehicles [1].

Emissions from a H_2-fueled engine can be reduced to a minimum by employing a suitably designed combustion process in lean-burn operation with exhaust gas recirculation [2]. However, a completely nitrogen-oxide-free combustion cannot be ensured at all operating points. Under certain conditions, nitrogen oxides can be emitted, mainly driven by the thermal formation mechanism occurring when the combustion temperature exceeds 2000 K, and for this reason, a deNO_x unit is required.

The use of a catalyzed exhaust after-treatment system using H_2 as a reducing agent would have the advantage that only one fuel needs to be carried on board both for propulsion and NO_x reduction, thus avoiding the devices for storage and injection of the urea

solution, required for the traditional NH_3-SCR for diesel engines. Moreover, compared to other reducing agents, hydrogen requires the lowest reaction temperature [3].

The NO_x reduction by H_2 produces, in theory, only elemental nitrogen and water [4].

$$2\,NO + 4\,H_2 + O_2 \rightarrow N_2 + 4\,H_2O \quad (1)$$

Nevertheless, the competitive reaction of hydrogen with the excess oxygen contained in the lean exhaust gas to directly produce water and the potential formation of N_2O, a strong greenhouse gas, can adversely affect the selectivity of the process [3].

Great efforts have been made recently to understand the relationship between the structure and reactivity of H_2-SCR catalysts, the most active being those based on noble metals such as platinum [3–5].

Noble metals-based catalysts are traditionally used for H_2-SCR due to the ability to decompose NO into adsorbed N and O and to generate active nitrate and NH_x^+ species from H_2 that is dissociatively adsorbed [3–5]. In fact, ammonium species are considered key reaction intermediates [6].

The use of a proper support for the active metal can largely affect the catalytic performance [7,8]. It has been reported that zeolite-supported Pt catalysts exhibited higher N_2 selectivity than metal oxide-supported counterparts; in particular, Pt/MFI provided the highest N_2 selectivity among zeolite-based catalysts [9,10]. The support significantly influences the dispersion and stability of the active element, as well as the catalyst's acidity [3–5]. Specifically, it was reported that Pt/ZSM-5 showed a larger amount of strong acid sites compared to Pt/SiO_2 or Pt/Al_2O_3, which, in turn, enhanced the specific catalytic activity [9]. Moreover, the location of Pt in the zeolite plays a crucial role: Pt^0 on the outer surface activates H_2, whereas Pt^{2+} within the zeolitic framework can adsorb NO_x as nitrite/nitrate species [6].

A further important drawback of Pt-based catalysts for the deNO_x process under excess O_2 is related to the production of significant amounts of NO_2 via the oxidation of NO that increases along with the reaction temperature, resulting in a relatively narrow operating window of Pt/zeolite catalysts [11,12]. Therefore, it is required to control and tune the oxidation ability of Pt to limit the NO_2 emissions. Park et al. [11] reported that a thermal ageing treatment of Pt/ZSM5 catalyst widened the temperature window of H_2-SCR by depressing the NO oxidation to NO_2, whereas Machida and Watanabe [13] reported enhancements of N_2 selectivity by adding various amounts of sodium to a 1 wt% Pt/ZSM5 catalysts.

In this work, we set out to investigate the H_2-SCR reaction of NO over a series of Pt/ZSM5 catalysts with limited metal loadings (0.1–1 wt%) and doped with Na (5–10 wt%) that was added to inhibit the NO oxidation activity. The effects of sodium addition on the main features of the original catalyst, such as the surface area and acidity, were studied to identify its inhibiting mechanism and the optimal loading that preserves the catalytic properties in the H_2-SCR. Eventually, an in situ DRIFTS study was performed to investigate the main surface species formed during the reaction both on the unpromoted and the Na-promoted catalysts and to assess their possible role in the reaction mechanism.

2. Results and Discussion

The parent commercial ZSM-5 zeolite did not show any activity for the H_2-SCR reaction of NO, confirming the results reported by others [14–16]. The addition of even a low amount of Pt (i.e., 0.1 wt%) activated the NO molecule, which was consumed in two different temperature ranges: from ca 80 to 200 °C and from 220 up to 450 °C (Figure 1). However, it must be noticed that for T > 200 °C, a NO_2 production was detected that increased along with the temperature and peaked at 380–410 °C depending on the

precious metal loading. As a consequence, only in the lower temperature range, the NO conversion was related to the occurrence of reaction (1) with high selectivity to N_2 (Figure 1b), which inevitably dropped to zero as soon as all of the H_2 in the feed was consumed (oxidized to H_2O).

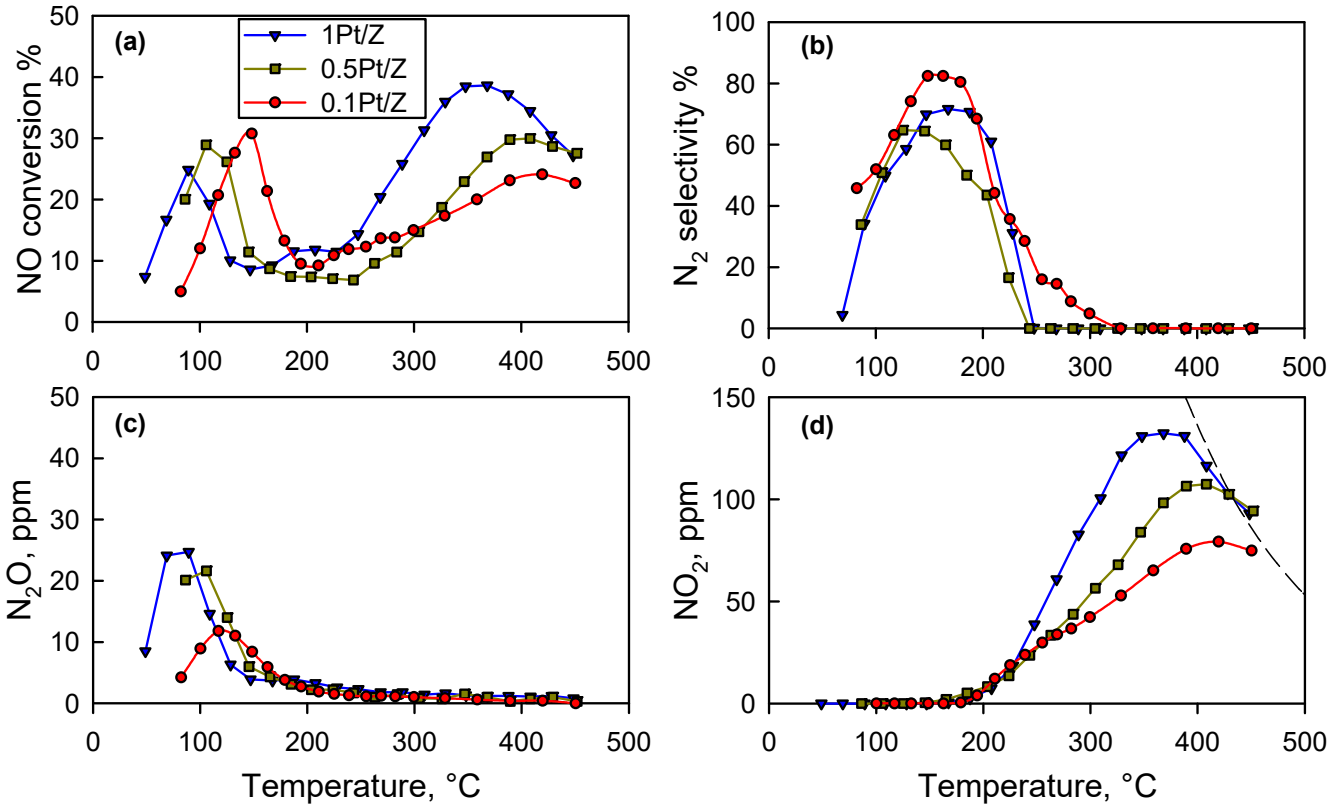


Figure 1. NO conversion (**a**), N_2 selectivity (**b**), and concentration of N_2O (**c**) and NO_2 (**d**) in the product stream during the H_2-SCR tests over 0.1Pt/Z, 0.5Pt/Z, and 1Pt/Z catalysts as a function of the reaction temperature. The dashed line in panel (**d**) corresponds to thermodynamic equilibrium data.

The maximum NO conversion in the low temperature range, was observed with 0.1Pt/Z catalyst at 144 °C and corresponded to 31%. This value is lower than others reported in the literature for zeolite-supported platinum catalysts (summarized in Table 1) even if a direct comparison is somehow precluded due to significant differences in the experimental conditions (particularly feed compositions and WHSV). The undesired formation of some N_2O was observed, as also reported by others [9]: it was higher for larger platinum loadings, and it peaked at the same temperature of the NO conversion with a direct impact on the process selectivity to N_2 (Figure 1b,c). Burch et al. [7,17] stated that N_2 and N_2O are produced by a parallel process involving a pre-adsorbed NO intermediate that can react with another adsorbed NO species to produce N_2O or with an adsorbed N atom to give N_2. The ratio between adsorbed hydrogen and adsorbed NO is also considered a key parameter in determining the N_2 selectivity with respect to N_2O [18]. According to these hypotheses, it can be argued that larger platinum clusters/nanoparticles can promote the adsorption of more NO intermediates close to each other, thus favouring their reaction to form N_2O.

As already mentioned, for T > 200 °C, the conversion of NO was mostly associated with its oxidation with O_2, producing NO_2. This agrees well with data reported in [13] showing that NO conversion to NO_2 increased between 150 and 300 °C with increasing concentrations of O_2 up to 10% in the feed. Hong et al. [14] investigated the NO oxidation activity of Pt/ZSM5 by feeding a mixture of NO and O_2 without H_2. They observed an

increasing NO_2 formation from 100 to about 250 °C catalyzed by platinum. As shown in Figure 1d, the oxidation of NO to NO_2 significantly increased along with the Pt content in the catalysts and became limited by the approach to the thermodynamic equilibrium [11,14] above 380–420 °C.

Table 1. Summary of activity data reported in the literature for the H_2-SCR over various Pt catalysts supported on zeolites.

Catalyst	Feed Composition	WHSV $dm^3\ g_{cat}^{-1}\ h^{-1}$	max NO_x Conv.%	N_2 Select.%	T_{Max} °C	Ref.
0.1Pt/ZSM5	300 ppm NO, 1200 ppm H_2, 5% O_2	200	31	81	144	[this work]
0.5Pt/ZSM5 from H_2PtCl_6	1000 ppm NO, 5000 ppm H_2, 10% O_2	60	~90	63	90	[6]
0.5Pt/ZSM5 from $Pt(NO_3)_2$	1000 ppm NO, 5000 ppm H_2, 10% O_2	60	~90	58	110	[6]
0.5Pt/ZSM5(h)	1000 ppm NO, 5000 ppm H_2, 10% O_2	60	~85	94	95	[14]
1Pt/ZSM5	910 ppm NO, 90 ppm NO_2, 5000 ppm H_2, 10% O_2	60	~70	78	130	[15]
0.5Pt/FER	910 ppm NO, 90 ppm NO_2, 5000 ppm H_2, 10% O_2	60	~85	100	110	[16]
0.2–0.5Pt/Y(ox)	1000 ppm NO, 5000 ppm H_2, 20% O_2	60	~80	80	100	[18]

Figure 2 reports the effect of the addition of 5 or 10% Na to the 0.1Pt/Z catalyst on the NO conversion as well as the undesired production of NO_2 and N_2O. The addition of 10% Na almost completely suppressed the NO_2 formation at high temperatures, but, unfortunately, it also strongly inhibited the overall NO conversion rate. On the other hand, the addition of 5% Na proved effective in depressing the undesired NO_2 formation at high temperatures as well as the N_2O formation (reaction (2)), which took place simultaneously with reaction (1) in the low-temperature range while preserving the activity towards the H_2-SCR. Such results align with those reported by Machida and Watanabe on similar catalysts [13], who found that Na doping could promote both NO conversion and N_2 selectivity. Burch and Coleman [17] observed a similar qualitative effect of Na doping on Pt/Al_2O_3 catalyst for H_2-SCR under lean conditions, although they did not detect the inhibition of N_2O formation, which was observed for the ZSM5-supported catalyst.

$$2\ NO + 4\ H_2 + 3/2\ O_2 \rightarrow N_2O + 4\ H_2O \quad (2)$$

Figure 3 presents the N_2 isotherms at 77 K for 0.1Pt/Z, 0.1Pt5Na/Z, and 0.1Pt10Na/Z catalysts. It can be observed that while 0.1Pt/Z and 0.1Pt5Na/Z preserved their typical shape characteristic of type I microporous materials (such as their parent ZSM5 support), the addition of 10% Na caused the almost complete loss of microporosity. The progressive reduction in the volume of micropores is clearly recognized in Figure 3b, where the area of the contribution of pores with a size <10 Å is roughly halved upon the addition of 5% Na, and it is basically zero upon the addition of 10% Na (Table 2).

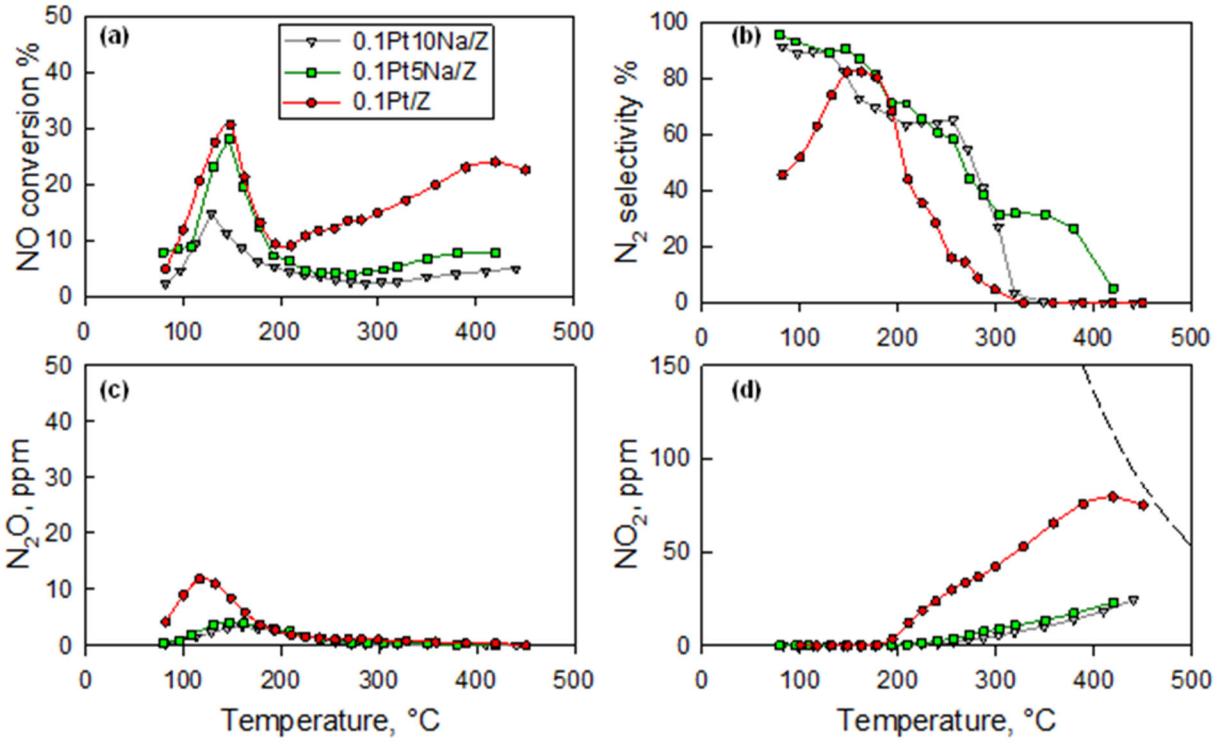


Figure 2. NO conversion (**a**), N_2 selectivity (**b**), and concentration of N_2O (**c**) and NO_2 (**d**) in the product stream during the H_2-SCR tests over 0.1Pt*y*Na/Z catalysts as a function of the reaction temperature. The dashed line in panel (**d**) corresponds to thermodynamic equilibrium data.

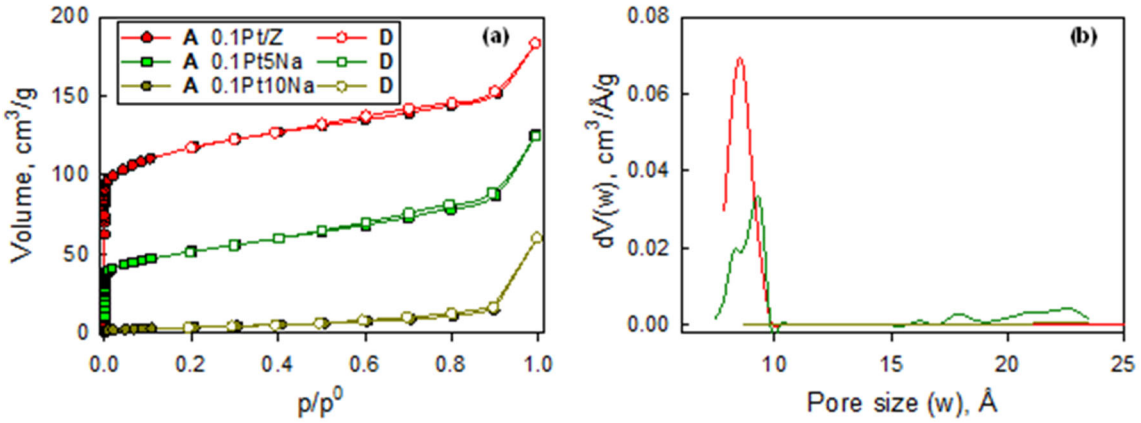


Figure 3. N_2 adsorption/desorption isotherms at 77 K (**a**) and corresponding pore size distribution analysis (**b**) for 0.1Pt*y*Na/Z catalysts.

Table 2. Textural properties of 0.1Pt*y*Na/Z catalysts and their parent H-ZSM5 support.

Catalyst	BET Area ($m^2\ g^{-1}$)	Micropore Volume ($cm^3\ g^{-1}$)
H-ZSM5	430	0.170
0.1Pt/Z	432	0.151
0.1Pt5Na/Z	184	0.076
0.1Pt10Na/Z	14	0.003

The parent zeolite, after thermal treatment at 550 °C, required to decompose the ammonium ion and obtain the zeolite in its H-form, showed a BET area of 430 $m^2\ g^{-1}$ [19]. The addition of 0.1% Pt did not change the textural properties or the crystalline structure

(PDF n. 04-13-2411), as confirmed by the comparison of the relevant XRD patterns shown in Figure 4. However, doping with 5% or 10% Na reduced the BET surface area of the samples down to 184 and to only 14 m^2 g^{-1}, respectively (Table 2). XRD analysis indicated the loss of surface area and porosity (particularly evident for the 0.1Pt10Na/Z catalyst) was not accompanied by any major modification of the crystalline structure of the parent zeolite, but rather it was due to pore blocking caused by the accumulation of Na-nitrate species giving a characteristic peak at 29.3° (PDF n. 079-2056) as shown in Figure 4.

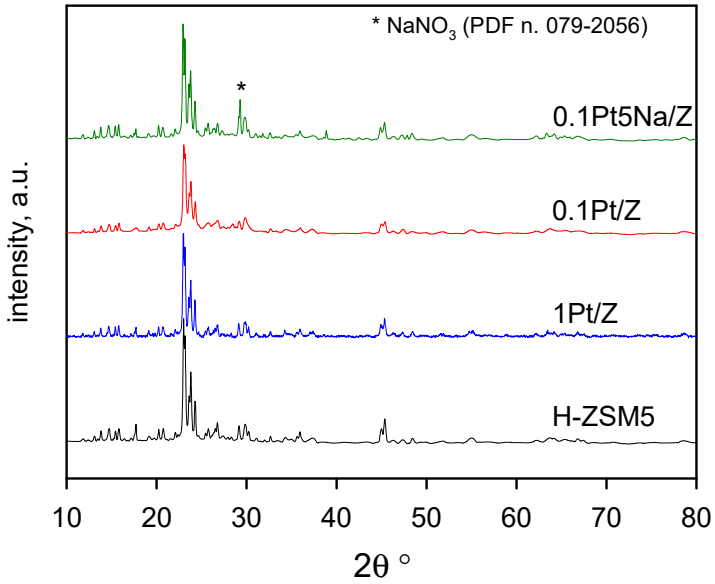


Figure 4. XRD patterns of 1Pt/Z, 0.1Pt/Z, and 0.1Pt5Na/Z catalysts compared to their parent H-ZSM5 support.

Accordingly, SEM analysis performed on the 0.1Pt5Na/Z catalyst (Figure 5) revealed the presence of needle-like crystals with a variable dimension (length 5–20 μm, width 1–5 μm) dispersed among irregular particles. The corresponding EDX mapping of Si, Al, and Na indicated that these crystals are mostly composed of sodium, thus corresponding to the $NaNO_3$ phase detected by XRD. On the other hand, the irregular particles mainly consisted of silicon and aluminum, clearly suggesting the assignment to the zeolite phase.

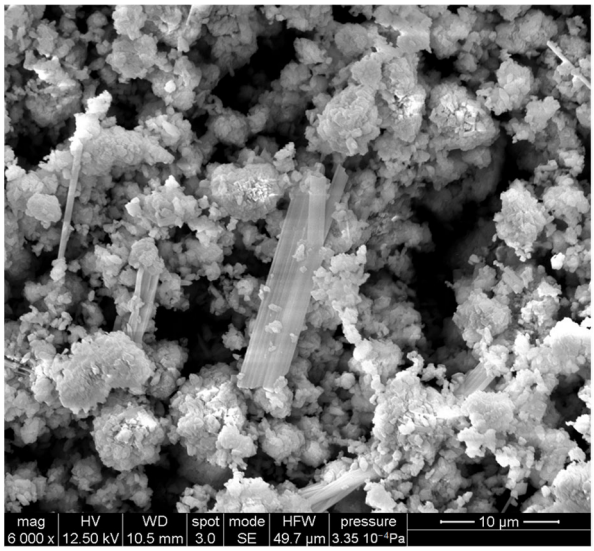


Figure 5. SEM image of the 0.1Pt5Na/Z catalyst showing the presence of some elongated $NaNO_3$ crystals.

A 49% platinum dispersion and an average particle size of 2.3 nm was evaluated for the 1Pt/Z catalyst using the H_2 chemisorption technique, whereas a correct estimation of dispersion was not possible for those materials with 0.1% Pt content due to the overall small quantities of H_2 chemisorbed. Therefore, a semi-quantitative analysis of platinum dispersion was performed by DRIFTS measurement of CO adsorption.

In Figure 6, the DRIFT spectra relevant to CO adsorption on the 0.1Pt/Z, 0.1Pt5Na/Z, and 1Pt/Z catalysts are presented. A single large and sharp band was detected at 2080 cm^{-1} for the 1Pt/Z sample, whereas very small bands were detected in the same region for the two catalysts with 0.1%Pt loading. The 0.1Pt/Z catalyst showed a broad band at 1935 cm^{-1} in addition to a small band at 2086 cm^{-1}. The band at 2080–2060 cm^{-1} was almost absent for the 0.1Pt5Na/Z sample, and one at 1930 cm^{-1} was significantly reduced compared to the Na-free counterpart.

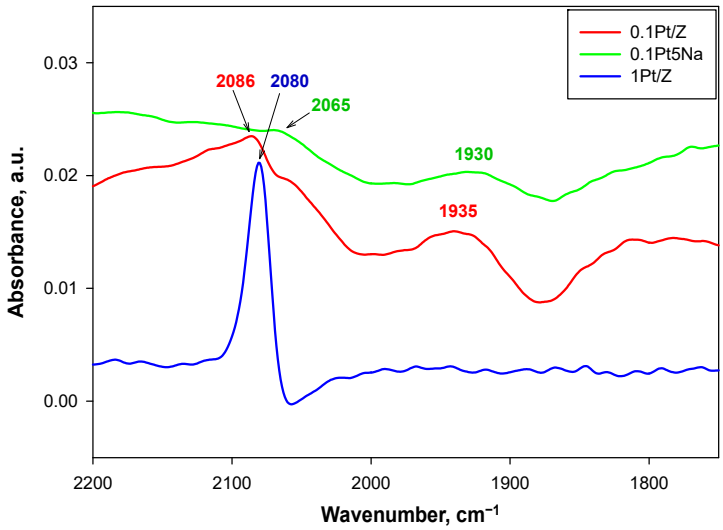


Figure 6. DRIFT spectra of CO adsorption on selected 1Pt/Z, 0.1Pt/Z, and 0.1Pt5Na/Z catalysts.

A band at 2075–2085 cm^{-1} has been commonly reported for CO adsorbed on Pt supported on zeolites and also other oxide supports [15,20–24].

For ν(CO) < 2100 cm^{-1}, it is assumed that CO is linearly adsorbed on Pt^0, whereas for ν(CO) > 2100 cm^{-1}, platinum is partially oxidized ($Pt^{\delta+}$) [22,24]. Therefore, it can be argued that platinum was completely reduced in all three catalysts after the H_2 pre-treatment. Nevertheless, the shift in the carbonyl band from 2086 to 2065 cm^{-1} for 0.1Pt/Z in the presence of sodium could indicate a lower oxidation state of platinum, as also suggested by Zhang et al. [15] for W-promoted Pt/ZSM5 catalysts. In good agreement with our results, Rivallan et al. [21] assumed for 2%Pt/ZSM5 that the band they detected at 2095 cm^{-1} was associated with CO on large Pt^0 particles with an average dimension of 6 nm, whereas a shift towards 2085 cm^{-1} indicated CO adsorption on smaller (about 2.5 nm) Pt^0 particles. Similarly, Han et al. [20] attributed the band at 2075 cm^{-1}, detected for platinum dispersed on L zeolite (load ranging from about 0.5 to 0.7%), to CO on Pt small clusters into zeolite pores.

The band at lower frequencies (1930–1935 cm^{-1}) is less commonly reported in the literature. Han et al. [20] reported that signals in the region 1900–1700 cm^{-1} can be assigned to bridged-bonded carbonyl species; in particular, they assigned a 1935–1920 cm^{-1} band to CO species between zeolite framework and Pt atoms. Consistently, Bazin et al. [22] reported that this low-frequency band was due to CO on very low coordinated Pt atoms strongly interacting with the support. Based on these assignments, it can be argued that at very low loadings (0.1% wt%), all the Pt strongly interacted with the ZSM5 support being

atomically dispersed. However, the accessibility of these Pt sites was somewhat limited by the further addition of sodium. At variance, when the metal loading was 1 wt%, the nature of the noble metal sites changed significantly due to the strong prevalence of small clusters with a characteristic size of ca 2–3 nm.

Figure 7 presents the NH_3-TPD profiles following ammonia saturation at room temperature. The characteristic traces for the parent zeolite and the two Pt/Z supported catalysts were almost overlapped regardless of the different Pt loadings, thus suggesting that the acid sites typical of the H-ZSM5 were preserved after the dispersion of the noble metal. Specifically, three main desorption events were detected, peaking at 110–120 °C, 215 °C and 440 °C. Hong et al. [14] reported that all Pt/ZSM-5 samples prepared by different methods showed two distinct NH_3 desorption peaks (below 300 °C and up to 600 °C) associated, respectively, to weakly acidic silanol groups and weak Lewis (or Brønsted) acid sites, and to the stronger acid sites. They also observed that the peaks at high temperatures became less intense after the introduction of platinum, indicating that some of the available strong acid sites were blocked by platinum. The same effect was reported by Yu et al. [25] for Pt/ZSM5 and Pt/ZSM35 but it was rather limited for our catalysts.

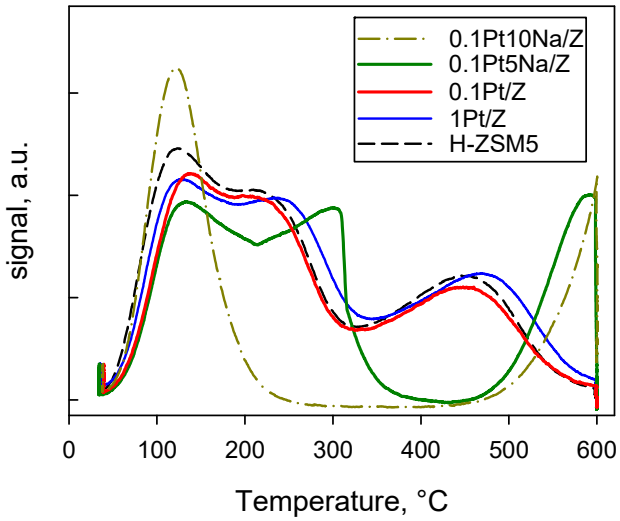


Figure 7. NH_3-TPD profiles recorded over *x*Pt*y*Na/Z catalysts and their parent H-ZSM5 support.

As expected, the addition of sodium strongly changed the acid properties of the catalyst: the most evident feature, common to both Na loadings, was the disappearance of the peak in the range 300–500 °C, representing the strong acid centres. However, for the 0.1Pt5Na/Z catalyst, most of the acid sites desorbing ammonia up to 300 °C were preserved, whereas they were totally neutralized at 10%Na load. For the 0.1Pt5Na/Z catalyst, new additional acid centres at 250–350 °C were formed whose nature was not defined.

Therefore, it seems that the target acid sites upon sodium addition are mainly those releasing ammonia in the 350–500 °C temperature range, as also observed by Hong et al. [14] for higher Pt loads. Zhang et al. [15] also observed a slight reduction in acid sites in the same temperature range upon tungsten addition to a 1Pt/ZSM5 catalyst. They associated this reduction with that of the silanols and Brønsted bands detected by FTIR, concluding that both platinum and tungsten occupied these positions. These certainly are the main targets of sodium in our catalysts, although other acid sites cannot be totally excluded. However, at 10 wt% of Na, medium acid strength sites were also neutralized with an evident negative impact on the SCR activity (see Figure 2a).

Hong et al. [14] found a rough correspondence between the total amount of acid sites and the NO conversion at 90 °C, corresponding to the maximum selectivity to N_2. Yu et al. [25] reported that at high Pt load, when the large platinum particles blocked acid

sites, the H_2-SCR dropped. Our results seem to suggest that weak and medium-strength acid sites (responsible for the first two partially overlapped peaks in NH_3-TPDs) can be involved in the H_2-SCR, whereas strong acid sites could promote the NO oxidation to NO_2.

Figure 8 presents the in situ DRIFTS spectra recorded over the 0.1Pt/Z, 1Pt/Z, and 0.1Pt5Na/Z catalysts at 30 °C under a $NO/O_2/Ar$ mixture and after H_2 was added to the gaseous feed at increasing temperatures up to 230 °C. These temperature levels were selected in order to investigate a range (60–130 °C) where reaction (1) mainly occurred and a temperature (230 °C) where NO oxidation to NO_2 took place.

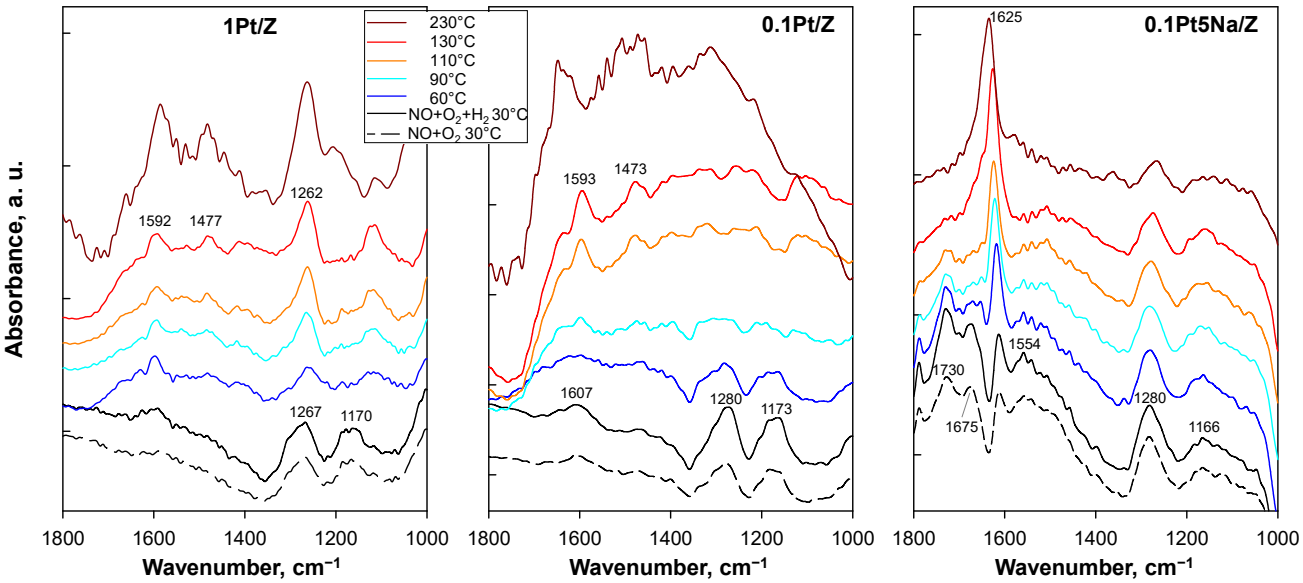


Figure 8. DRIFT spectra of 1Pt/Z, 0.1Pt/Z, and 0.1Pt5Na/Z after $NO+O_2$ adsorption at 30 °C followed by reaction in $NO+O_2+H_2$ at increasing temperatures. Further experimental details are reported in Section 3.

Two bands at 1267–1280 cm^{-1} and at 1170–1173 cm^{-1} were present in the spectra of both 0.1Pt/Z and 1Pt/Z, along with a very small signal at ca 1600 cm^{-1} after the adsorption of $NO+O_2$ at 30 °C (dashed lines). The intensity of these signals did not change significantly regardless of the Pt loading, and they were also observed in the parent H-ZSM5, suggesting they can be assigned to NO on the zeolite rather than on platinum. The simultaneous presence of H_2 at this temperature increased the intensity of all these bands. New bands at 1593 cm^{-1}, with a shoulder at 1625 cm^{-1} more evident for 0.1Pt/Z, and 1473 cm^{-1} appeared by increasing the temperature up to 130 °C. Interestingly, the intensity of the band at 1267–1280 cm^{-1} increased along with the temperature for the 1Pt/Z catalyst, whilst this feature disappeared for the sample with a low platinum content. Moreover, the signal at 1170 cm^{-1} shifted towards lower wavenumbers for 1Pt/Z.

At 230 °C, when the NO oxidation prevailed on the SCR, different bands were detected on both catalysts: for 0.1Pt/Z at 1650, 1480, and 1312 cm^{-1} and for 1Pt/Z at 1586 and 1480 cm^{-1} whereas a shoulder at 1203 cm^{-1} appeared on the sharp band peaked at 1260 cm^{-1}, already present at lower temperatures.

Na-doping strongly affected the main features of the DRIFT spectra. In addition to the low-frequency bands (at 1280 and 1166 cm^{-1}) also observed for the unpromoted catalysts, which confirmed the major role of the zeolite support in this spectral region, bands at 1554, 1675, and 1730 cm^{-1} were detected, together with a sharp one at 1625 cm^{-1} becoming even more intense at higher temperatures. A quite intense band at 1625 cm^{-1} was also detected by Zhang et al. [15] upon NO or $NO+O_2$ adsorption on Pt/ZSM5 catalysts, either with or without tungsten-doping, whilst its intensity was reduced under the complete $NO-H_2-O_2$

mixture for the W-containing catalyst. A band at this position was previously reported by Szanyi and Paffett [26] for NaH-ZSM5, and it was found to increase with the reaction time, thus suggesting it was due to nitrate species bound to Na^+ ions in cationic positions. The possible contribution of bulk sodium nitrate from the crystallites detected by XRD analysis, expected at ca 1270 and 1635 cm^{-1} [27], must be excluded because it was deleted by the background ratioing operation. As a consequence, this feature should represent nitrate species formed upon exposure to the NO-containing mixture and can be definitively associated with the presence of sodium for our catalysts since the same band was very weak for the unpromoted sample.

The presence of H_2 in the feed mixture did not significantly modify the main signals for the Na-doped catalysts; however, the temperature increase resulted in the disappearance of the bands at 1675, 1730, and 1554 cm^{-1}, as well as a reduction in the intensity of the signals at 1280 and 1166 cm^{-1}.

The attribution of the main bands of adsorbed NO_x species was reported by Morrow et al. [28] for Pt/SiO_2. They found that the intensity of bands at 1785 and 1620 cm^{-1}, assigned to linear and bent or bridged NO on Pt, respectively, decreased upon O_2 introduction, replaced by a band at 1710 cm^{-1} and one at 1545 cm^{-1} assigned to linear NO and bidentate nitrate species on oxidized Pt, respectively. A band at 1540 cm^{-1} was also assigned to adsorbed N_2O_3 dimer on the zeolite, which was detected by Szanyi et al. [29] on Na-Y upon the addition of O_2 to gaseous NO, suggesting these are oxidized adsorbed species. The low-frequency bands were assigned by the same authors to nitrate species on the support.

On this basis, the formation of a band around 1590 cm^{-1} by increasing the temperature in the presence of O_2 suggests that some platinum could be oxidized under excess O_2, even if in the co-presence of H_2. Moreover, the reduction in the bands at 1785 and 1675 cm^{-1}, coupled with the growth of the 1625 cm^{-1} signal, which remained stable upon H_2 addition at increasing temperatures, suggests the formation of a species which does not evolve into NO_2.

The band at 1473–1477 cm^{-1}, well detected for both unpromoted catalysts in the presence of H_2 at high temperature, was attributed to NH_4^+ (on Brønsted acid sites) produced by the reduction in the nitrous species [16,18]. Eventually, the bands identified only for the Na-containing catalyst in the 1800–700 cm^{-1} range were assigned to NO dimers [13,30].

At 230 °C, a temperature promoting the oxidation of NO to NO_2, the main features of the spectrum did not markedly change for the Na-promoted catalyst, whereas bands similar but with a worse signal/noise ratio were detected for both 0.1Pt/Z and 1Pt/Z.

In order to better identify the adsorbed NO_x species involved in the SCR reaction, H_2 was introduced at 100 °C, a temperature where the SCR prevails after NO/O_2 was pre-adsorbed on the catalyst. In Figure 9, the corresponding DRIFT spectra are reported for the 0.1Pt/Z, 1Pt/Z, and 0.1Pt5Na/Z catalysts. The same experiments performed over the parent H-ZSM5 revealed low-intensity broad bands in the regions 1800–1600, 1600–1400, and 1400–1200 cm^{-1} [31] that did not change upon H_2 introduction, thus confirming the key role of platinum to activate the H_2-SCR reaction.

As for the spectra recorded under reaction conditions, the features of 0.1PtNa/Z were markedly different from those of the unpromoted catalysts. Following exposure to NO/O_2, both unpromoted samples showed a broad band peaked at 1723–1730 cm^{-1} with a shoulder at 1819–1826 cm^{-1} that can be attributed to adsorbed nitrate species on Pt [13] or to NO dimer [14] also on H-ZSM5 [29,30]. These species were not detected when NO, O_2, and H_2 were simultaneously co-fed at a similar temperature level, and this could indicate their steady-state consumption under reaction conditions. Two further bands at 1590–1595 and

1625–1630 cm^{-1} were clearly detected over 1Pt/Z as well as 0.1Pt/Z, though with lower intensity. At variance, a large broad band peaked at ca 2100 cm^{-1} for 0.1Pt/Z, decreased with platinum loading and even more with Na addition. This feature was assigned to 2O-NO^+ generated by the reaction between N_2O_3 (from NO+NO_2) and protons of H-ZSM5 when it is exposed to NO+O_2 [30]. The decrease in this band in 1Pt/Z and 0.1Pt5Na/Z indicates the disappearance of acid centres related to the dispersion of metals and can be associated with the loss of weak acid centres detected in TPD experiments.

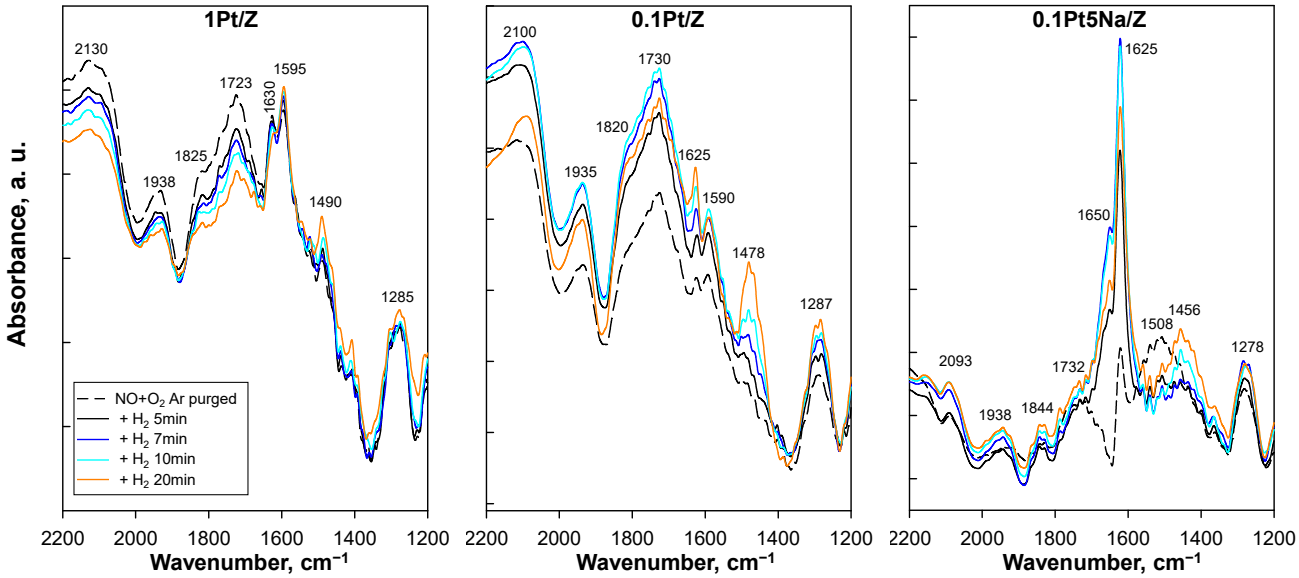


Figure 9. DRIFT spectra of 1Pt/Z, 0.1Pt/Z, and 0.1Pt5Na/Z purged in Ar after NO+O_2 adsorption at 100 °C and during the subsequent exposure to H_2 in Ar at the same temperature for increasing times on stream. Further experimental details are reported in Section 3.

The addition of H_2 at 100 °C did not modify the large band in the range 1700–1850 cm^{-1} for 0.1Pt/Z, whereas it progressively reduced it along with the time on stream for 1Pt/Z suggesting these species could be involved in the undesired formation of N_2O. Nevertheless, it must be reiterated that the 1Pt/Z catalyst activated the SCR reaction at a lower temperature. The other bands did not change significantly with time on stream, excluding the increase in the small band at ca 1490 cm^{-1} along with the small signal at 1625 cm^{-1}, highlighting a major role of ammonium as a reaction intermediate at low Pt load.

As already observed for the experiments under steady-state reaction conditions, the band at 1625 cm^{-1} represented the dominant band in the spectrum of 0.1Pt5Na/Z, and it strongly increased upon H_2 addition with ToS up to 10 min along with a shoulder at 1650 cm^{-1}, associated with linear NO on Pt [28]. Furthermore, a band initially present at 1510 cm^{-1} in the absence of H_2 was gradually replaced by a new band at 1450 cm^{-1}, suggesting that bidentate nitrate species on oxidized Pt were transformed into adsorbed ammonium species, which then produced molecular nitrogen according to the reaction:

$$NOx\ (ad) + NH_4+ \rightarrow N_2 + H_2O + H+ \quad (3)$$

as proposed by Wang et al. [6]. The effect of H_2 on all the other signals was negligible for the Na-promoted catalyst.

It must be noticed that the ammonium band was well detectable for the two catalysts providing the best N_2 selectivity whereas the formation of ammonium appeared to be inhibited at high Pt loading.

In conclusion, it can be argued that the catalyst with a low Pt content (and high dispersion) activates the reaction path involving the formation of nitrates (likely dimers) on highly dispersed platinum associated with the band in the 1590–1510 cm^{-1} region, which can easily evolve into ammonium intermediate. Moreover, the neutralization of the strong acid sites provided by Na-doping (at 5 wt%) can suppress the undesired NO oxidation without affecting the Pt activity or the low- and medium-strength acidity, which plays an important role in the activation of the H_2-SCR reaction. The selective reaction path is indeed still preserved at a low Na load, as shown by the detection of active nitrate and ammonium-adsorbed species on this promoted catalyst.

3. Materials and Methods

3.1. Catalysts Synthesis

A commercial ZSM5 powder with a SiO_2/Al_2O_3 ratio = 23 was supplied by Zeolyst (Kansas City, KS, USA) in its ammonium form. The zeolite support was preliminarily treated for 2 h at 550 °C in the air to obtain the corresponding H-form, and then it was impregnated with aqueous solutions of Tetra-ammine-platinum(II) chloride hydrate (Sigma Aldrich, Steinheim, Germany) (98% purity) to obtain nominal precious metal loadings of 0.1, 0.5, and 1 wt% The samples were dried at 120 °C and then calcined in air at 400 °C for 2 h. Na doping on the 0.1%Pt/ZSM5 catalyst was achieved by impregnation with aqueous solutions of sodium nitrate (Sigma Aldrich 99.0% purity) targeting a nominal loading of Na equal to 5 or 10 wt%, followed by a novel calcination step at 400 °C under air.

The catalysts were labelled as *x*Pt*y*Na/Z, where *x* is the nominal weight percentage of Pt, *y* is that of Na, and Z is the ZSM5 support.

3.2. Catalytic Tests

The catalytic tests were carried out in a lab-scale rig at atmospheric pressure using 0.125 g of catalyst (180–200 mm particle size) loaded in a tubular fixed bed quartz reactor (inner diameter = 10 mm), which was externally heated by an electrical tubular furnace. The inlet gas feed to the reactor contained 300 ppmv NO (NO_2 impurity < 3 ppmv), 1200 ppm H_2, 5% O_2 and He as balance: it was obtained by mixing gas streams from high purity cylinders (NO in He, H_2 in He, O_2, He) regulated by independent mass flow controllers (BROOKS, Greenville, PA, USA) MFC SLA5850S) to achieve a total flow rate of 25 $Sdm^3\ h^{-1}$. The operating temperature ranged from 75 to 450 °C.

Gas analysis of NO_x was performed by an Emerson X-Stream XEGP continuous analyzer with independent detectors (NO and N_2O (ND-IR), NO_2 (UV)). Water produced by the reaction was removed from the gas stream using a Sycapent™ (P_2O_5) trap before entering the NO_x analyzer.

3.3. Catalysts Characterization

X-ray diffraction patterns were recorded on ground samples using a Rigaku (Tokyo, Japan) Miniflex 600 diffractometer with Cu Kα radiation (0.154 nm wavelength) in a 2θ range of 10–80°, with a step of 0.01° and 10°/min counting time. Background correction, fitting, and peak attribution were performed using SmartLab Studio II software.

Specific surface area measurements and micro- and meso-pore analysis were performed in an Autosorb 1-C (Quantachrome, Boynton Beach, FL, USA) through N_2 adsorption at 77 K after degassing the samples for 2 h at 150 °C. The specific surface area and the pore size distribution were evaluated by the BET and NLDFT methods (cylindrical pore equilibrium model), respectively.

Scanning electron microscopy was performed with an FEI (Hillsboro, OR, USA) Inspect instrument equipped with an EDAX-Energy Dispersive Detector (EDS) for the elemental analysis.

H_2 chemisorption analysis was carried out using an Autosorb iQ (Anton Parr, Graz, Austria) pre-reducing the sample (about 1 g) at 400 °C under a flow of pure H_2 for 1 h, then evacuating for 2 h at the same temperature and cooling down under vacu (Atlantaum to 40 °C where H_2 adsorption was performed.

NH_3 temperature programmed desorption (TPD) tests were performed with a Micromeritics (Atlanta, GA, USA) AutoChem 2020 equipped with a TC detector. Samples were pre-treated in situ under airflow at 400 °C for 1 h; thereafter, 5% NH_3/He mixture (50 cm^3 min^{-1}) was passed through the sample at room temperature. After saturation and purge (30 min) under pure He at room temperature, the sample was heated up to 600 °C at 10 °C min^{-1}.

DRIFTS experiments of CO adsorption were performed in a Perkin Elmer (Hopkinton, MA, USA) Spectrum 3 spectrometer equipped with a liquid-N_2 cooled MCT detector at 4 cm^{-1} resolution, averaging over 64 scans. Powdered samples were loaded in a heated chamber equipped with a ZnSe window (DRIFT PiKe, Madison, WI, USA) and pre-treated in situ under 25% H_2/Ar flow at 400 °C for 2 h followed by 20 min Ar purging and cooling down to 30 °C where a background spectrum was recorded. Thereafter, a 5% CO/N_2 mixture was fluxed for 15 min into the cell, and after purging again, a spectrum was recorded and rationed against the background.

3.4. In Situ DRIFTS Experiments

Two kinds of in situ DRIFTS experiments were performed in the same instrumental set-up previously described to investigate the reaction mechanism of the H_2-SCR over the catalysts that were pre-treated in Ar at 400 °C for 1 h. In the first set of (steady-state) experiments, a NO/O_2/Ar mixture (300 ppm NO, 5%O_2) was contacted with the catalyst at 30 °C for 30 min, and a spectrum was recorded. Then, H_2 (1200 ppm) was added to the gas feed containing NO and O_2, and a new spectrum was recorded after stabilization for 15 min. Eventually, the temperature was increased stepwise up to 230 °C, and relevant spectra were recorded at 60, 90, 110, 130, and 230 °C.

For the second set of (transient) experiments, each pre-treated catalyst was first contacted at 100 °C with the same NO/O_2/Ar mixture, and a spectrum was recorded after 15 min of purging with Ar. Thereafter, the feed gas to the DRIFT chamber was switched to a 1200 ppm H_2/Ar mixture, and spectra were continuously recorded at increasing time on stream (ToS) while the temperature was kept constant. For each test, the background spectrum corresponded to that of the pre-treated catalyst under Ar flow at the specific temperature level.

4. Conclusions

Platinum was supported on ZSM5 with a nominal content ranging from 0.1 to 1 wt%, and the resulting catalysts were tested for the Selective Catalytic Reduction of NO with H_2 under excess O_2, targeting the abatement of NO_x emissions from H_2-fueled internal combustion engines.

The Pt/ZSM5 catalysts promoted the NO conversion already at a very low temperature in the range of 50–150 °C, but beyond this threshold, the oxidation of NO to NO_2 activated by platinum itself prevailed over the desired SCR.

Reducing the noble metal loading down to as low as 0.1 wt% enhanced the maximum NO abatement performance achieved by the SCR reaction while shifting the optimal operating temperature range by 60–70 °C up to ca 150 °C.

To inhibit the unwanted NO oxidation reactions, the 0.1%Pt/ZSM5 catalyst was further promoted with Na (5 or 10 wt%). Notably, doping by sodium at mid-low loadings strongly inhibited NO oxidation to either NO_2 as well as N_2O in the entire temperature range explored, while it slightly affected the H_2-SCR activity. In particular, Na addition totally neutralized strong acid sites while preserving most of the low–medium-strength acid sites likely involved in the H_2-SCR reaction.

In situ DRIFTS experiments carried out under reaction conditions identified different nitrate species formed on the zeolite surface, on Pt sites, and on sodium. The results suggested that the selective H_2-SCR reaction path was activated by highly dispersed platinum and passed through the formation of ammonium intermediates, which were still detected over the Na-promoted catalyst with a moderate sodium loading while they disappeared at high platinum loadings.

These results pave the way to further optimization of the catalytic formulation via precise control of both content and dispersion of either the precious metal or the alkali promoter within the zeolite framework.

Author Contributions: Conceptualization, L.L. and S.C.; methodology, L.L. and S.C.; formal analysis, E.M.C.; investigation, E.M.C. and M.E.F.; funding acquisition, L.L.; data curation, E.M.C. and M.E.F.; writing—original draft preparation, L.L.; writing—review and editing, L.L. and S.C. All authors have read and agreed to the published version of the manuscript.

Funding: This research was funded by the European Union—NextGeneration EU from the Italian Ministry of Environment and Energy Security POR H2 AdP MMES/ENEA with involvement of CNR and RSE, PNRR—Mission 2, Component 2, Investment 3.5 "Ricerca e sviluppo sull'idrogeno", CUP: B93C22000630006. E.M. Cepollaro acknowledges funding from the European Union—NextGenerationEU under the National Recovery and Resilience Plan (NRRP), Mission 4 Component 2 Investment 3.1, Project. Code: IR0000027−CUP: B33C22000710006−iENTRANCE@ENL: Infrastructure for Energy TRAnsition aNd Circular Economy @Euro-Nanolab.

Data Availability Statement: The raw data supporting the conclusions of this article will be made available by the authors upon request.

Acknowledgments: The authors would like to thank Andrea Capuozzo for XRD and porosimetric analysis.

Conflicts of Interest: The authors declare no conflicts of interest.

References

1. Verhelst, S.; Wallner, T. Hydrogen-fueled internal combustion engines. *Prog. Energy Combust. Sci.* **2009**, *35*, 490–527. [CrossRef]
2. Koch, D.; Sousa, A.; Bertram, D. *H_2-Engine Operation with EGR-Achieving High Power and High Efficiency Emission-Free Combustion*; SAE Technical Paper 2019-01-2178; SAE International: Warrendale, PA, USA, 2019.
3. Guan, Y.; Liu, Y.; Lv, Q.; Wang, B.; Che, D. Review on the selective catalytic reduction of NO_x with H_2 by using novel catalysts. *J. Environ. Chem. Eng.* **2021**, *9*, 106770. [CrossRef]
4. Hu, Z.; Yang, R.T. 110th Anniversary: Recent Progress and Future Challenges in Selective Catalytic Reduction of NO by H_2 in the Presence of O_2. *Ind. Eng. Chem. Res.* **2019**, *58*, 10140–10153. [CrossRef]
5. Savva, P.G.; Costa, C.N. Hydrogen Lean-DeNO_x as an Alternative to the Ammonia and Hydrocarbon Selective Catalytic Reduction (SCR). *Catal. Rev. Sci. Eng.* **2011**, *53*, 91–151. [CrossRef]
6. Wang, X.; Wang, X.; Yu, H.; Wang, X. The functions of Pt located at different positions of HZSM-5 in H_2-SCR. *Chem. Eng. J.* **2019**, *355*, 470–477. [CrossRef]
7. Burch, R.; Coleman, M.D. An investigation of the $NO/H_2/O_2$ reaction on noble-metal catalysts at low temperatures under lean-burn conditions. *Appl. Catal. B Environ.* **1999**, *23*, 115–121. [CrossRef]
8. Farhan, S.M.; Wang, P.; Chen, Z.; Yin, J. Innovative catalysts for the selective catalytic reduction of NO_x with H_2: A systematic review. *Fuel* **2024**, *355*, 129364. [CrossRef]
9. Shibata, J.; Hashimoto, M.; Shimizu, K.; Yoshida, H.; Hattori, T.; Satsuma, A. Factors Controlling Activity and Selectivity for SCR of NO by Hydrogen over Supported Platinum Catalysts. *J. Phys. Chem. B* **2004**, *108*, 18327–18335. [CrossRef]

10. Liu, Z.; Li, J.; Woo, S.I. Recent advances in the selective catalytic reduction of NO_x by hydrogen in the presence of oxygen. *Energy Environ. Sci.* **2012**, *5*, 8799–8814. [CrossRef]
11. Park, D.C.; Moon, S.; Song, J.H.; Kim, H.; Lee, E.; Lim, Y.H.; Kim, D.H. Widening the operating window of Pt/ZSM-5 catalysts for efficient NO_x removal in H_2-SCR: Insights from thermal aging. *Catal. Today* **2024**, *425*, 114318. [CrossRef]
12. Despres, J.; Koebel, M.; Elsener, M.; Wokaun, A. *Investigation of the Oxidation of NO Over Platinum Catalysts*; Paul Scherrer Institut: Würenlingen, Switzerland, 2002.
13. Machida, M.; Watanabe, T. Effect of Na-addition on catalytic activity of Pt-ZSM-5 for low-temperature NO–H_2–O_2 reactions. *Appl. Catal. B Environ.* **2004**, *52*, 281–286. [CrossRef]
14. Hong, Z.; Wang, Z.; Chen, D.; Sun, Q.; Li, X. Hollow ZSM-5 encapsulated Pt nanoparticles for selective catalytic reduction of NO by hydrogen. *Appl. Surf. Sci.* **2018**, *440*, 1037–1046. [CrossRef]
15. Zhang, X.; Wang, X.; Zhao, X.; Xu, Y.; Liu, Y.; Yu, Q. Promotion effect of tungsten on the activity of Pt/HZSM-5 for H_2-SCR. *Chem. Eng. J.* **2015**, *260*, 419–426. [CrossRef]
16. Yang, S.; Wang, X.; Chu, W.; Song, Z.; Zhao, S. An investigation of the surface intermediates of H_2-SCR of NO_x over Pt/H-FER. *Appl. Catal. B Env.* **2011**, *107*, 380–385. [CrossRef]
17. Burch, R.; Coleman, M.D. An Investigation of Promoter Effects in the Reduction of NO by H_2 under Lean-Burn Conditions. *J. Catal.* **2002**, *208*, 435–447. [CrossRef]
18. Zhang, X.; Wang, X.; Zhao, X.; Xu, Y.; Gao, H.; Zhang, F. An investigation on N_2O formation route over Pt/HY in H_2-SCR. *Chem. Eng. J.* **2014**, *252*, 288–297. [CrossRef]
19. Cepollaro, E.M.; Botti, R.; Franchin, G.; Lisi, L.; Colombo, P.; Cimino, S. Cu/ZSM5-Geopolymer 3D-Printed Monoliths for the NH_3-SCR of NO_x. *Catalysts* **2021**, *11*, 1212. [CrossRef]
20. Han, W.-J.; Kooh, A.B.; Hicks, R.F. Infrared spectroscopy of carbon monoxide adsorbed on Pt/L zeolite. *Catal. Lett.* **1993**, *18*, 193–208. [CrossRef]
21. Rivallan, M.; Seguin, E.; Thomas, S.; Lepage, M.; Takagi, N.; Hirata, H.; Thibault-Starzyk, F. Platinum sintering on H-ZSM-5 Followed by Chemometrics of CO Adsorption and 2D Pressure-Jump IR Spectroscopy of Adsorbed Species. *Angew. Chem. Int. Ed.* **2010**, *49*, 785–789. [CrossRef]
22. Bazin, P.; Saur, O.; Lavalley, J.C.; Daturi, M.; Blanchard, G. FT-IR study of CO adsorption on Pt/CeO_2: Characterisation and structural rearrangement of small Pt particles. *Phys. Chem. Chem. Phys.* **2005**, *7*, 187–194. [CrossRef]
23. Chakarova, K.; Hadjiivanov, K.; Atanasova, G.; Tenchev, K. Effect of preparation technique on the properties of platinum in NaY zeolite: A study by FTIR spectroscopy of adsorbed CO. *J. Mol. Catal. A Chem.* **2007**, *264*, 270–279. [CrossRef]
24. Chakarova, K.; Mihaylov, M.; Hadjiivanov, K. FTIR spectroscopic study of CO adsorption on Pt–H–ZSM-5. *Microporous Mesoporous Mater.* **2005**, *81*, 305–312. [CrossRef]
25. Yu, Q.; Richter, M.; Kong, F.; Li, L.; Wu, G.; Guan, N. Selective catalytic reduction of NO by hydrogen over Pt/ZSM-35. *Catal. Today* **2010**, *158*, 452–458. [CrossRef]
26. Szanyi, J.; Paffett, M.T. The Adsorption of NO and Reaction of NO with O_2 on H-, NaH-, CuH- and Cu-ZSM-5: An in Situ FTIR Investigation. *J. Catal.* **1996**, *164*, 232–245. [CrossRef]
27. Hammad, T.M. Infrared absorption spectra studies in ($NaNO_3$–$NaNO_2$) system. *Ann. Phys.* **2002**, *11*, 435–441. [CrossRef]
28. Morrow, B.A.; Chevrier, J.P.; Moran, L.E. An Infrared Study of the Adsorption of NO on Silica-Supported Platinum over a Wide Temperature Range. *J. Catal.* **1985**, *91*, 208–215. [CrossRef]
29. Szanyi, J.; Kwak, J.H.; Moline, R.A.; Peden, C.H.F. The adsorption of NO_2 and the NO+O_2 reaction on Na-Y,FAU: An in situ FTIR investigation. *Phys. Chem. Chem. Phys.* **2003**, *5*, 4045–4051. [CrossRef]
30. Hadjiivanov, K.; Klissurski, D.; Ramis, G.; Busca, G. Fourier transform IR study of NO_x adsorption on a CuZSM-5 DeNOx catalyst. *Appl. Catal. B Environ.* **1996**, *7*, 251–267. [CrossRef]
31. Penkova, A.; Hadjiivanov, K.; Mihaylov, M.; Daturi, M.; Saussey, J.; Lavalley, J.-C. FTIR Spectroscopic Study of Low Temperature NO Adsorption and NO + O_2 Coadsorption on H−ZSM-5. *Langmuir* **2004**, *20*, 5425–5431. [CrossRef]

Disclaimer/Publisher's Note: The statements, opinions and data contained in all publications are solely those of the individual author(s) and contributor(s) and not of MDPI and/or the editor(s). MDPI and/or the editor(s) disclaim responsibility for any injury to people or property resulting from any ideas, methods, instructions or products referred to in the content.